



HAL
open science

Annular phased array transducer for preclinical testing of anti-cancer drug efficacy on small animals

Tamara Kujawska, Wojciech Secomski, Michal Byra, Michiel Postema,
Andrzej Nowicki

► **To cite this version:**

Tamara Kujawska, Wojciech Secomski, Michal Byra, Michiel Postema, Andrzej Nowicki. Annular phased array transducer for preclinical testing of anti-cancer drug efficacy on small animals. *Ultrasonics*, 2017, 76, pp.92-98. 10.1016/j.ultras.2016.12.008 . hal-03192798

HAL Id: hal-03192798

<https://hal.science/hal-03192798>

Submitted on 15 Apr 2021

HAL is a multi-disciplinary open access archive for the deposit and dissemination of scientific research documents, whether they are published or not. The documents may come from teaching and research institutions in France or abroad, or from public or private research centers.

L'archive ouverte pluridisciplinaire **HAL**, est destinée au dépôt et à la diffusion de documents scientifiques de niveau recherche, publiés ou non, émanant des établissements d'enseignement et de recherche français ou étrangers, des laboratoires publics ou privés.



Distributed under a Creative Commons Attribution - NonCommercial - NoDerivatives 4.0 International License

1
2
3
4
5
6
7
8
9
10
11
12
13
14
15
16
17
18
19
20
21
22
23
24
25
26

Annular phased array transducer for preclinical testing of anti-cancer drug efficacy on small animals

Tamara Kujawska*, Wojciech Secomski, Michał Byra, Michiel Postema, Andrzej Nowicki

Department of Ultrasound, Institute of Fundamental Technological Research,
Polish Academy of Sciences, Pawińskiego 5b, 02-106 Warsaw, Poland

*Corresponding author:

Tamara Kujawska

Department of Ultrasound, Institute of Fundamental Technological Research of the
Polish Academy of Sciences, Pawińskiego 5b, 02-106 Warsaw, Poland

+48 22 826 12 81 ext 178

E-mail: *tkujaw@ippt.pan.pl*

1 **Abstract.**

2 A technique using pulsed High Intensity Focused Ultrasound (HIFU) to destroy deep-seated solid
3 tumors is a promising noninvasive therapeutic approach. A main purpose of this study was to
4 design and test a HIFU transducer suitable for preclinical studies of efficacy of tested, anti-cancer
5 drugs, activated by HIFU beams, in the treatment of a variety of solid tumors implanted to various
6 organs of small animals at the depth of the order of 1-2 cm under the skin. To allow focusing of the
7 beam, generated by such transducer, within treated tissue at different depths, a spherical, 2-MHz,
8 29-mm diameter annular phased array transducer was designed and built. To prove its potential for
9 preclinical studies on small animals, multiple thermal lesions were induced in a pork loin *ex vivo* by
10 heating beams of the same: 6W, or 12W, or 18W acoustic power and 25mm, 30mm, and 35mm
11 focal lengths. Time delay for each annulus was controlled electronically to provide beam focusing
12 within tissue at the depths of 10mm, 15mm, and 20mm. The exposure time required to induce local
13 necrosis was determined at different depths using thermocouples. Location and extent of thermal
14 lesions determined from numerical simulations were compared with those measured using
15 ultrasound and magnetic resonance imaging techniques and verified by a digital caliper after cutting
16 the tested tissue samples. Quantitative analysis of the results showed that the location and extent of
17 necrotic lesions on the magnetic resonance images are consistent with those predicted numerically
18 and measured by caliper. The edges of lesions were clearly outlined although on ultrasound images
19 they were fuzzy. This allows to conclude that the use of the transducer designed offers an effective
20 noninvasive tool not only to induce local necrotic lesions within treated tissue without damaging the
21 surrounding tissue structures but also to test various chemotherapeutics activated by the HIFU
22 beams in preclinical studies on small animals.

23

24

25 **Keywords:** spherical annular phased array transducer, pulsed HIFU beam, electronically adjustable
26 focal length, local tissue heating, thermal ablation, necrotic lesion.

1 **1. Introduction.**

2 Pulsed High Intensity Focused Ultrasound (HIFU) is a promising non-invasive technique, i. a.
3 for the thermo-ablative treatment of solid tumors located deep under the skin [1-2]. The depth at
4 which the thermal lesion is desired to form depends on the geometry and acoustic parameters of the
5 transducer as well as on geometry and acoustic and thermal properties of propagation media used.
6 An advantage of this technique is its ability to provide non-invasive damage of a small volume
7 within tissue without damaging adjacent structures. This volume is determined by the dimensions of
8 the ellipsoidal focal spot of the heating beam used and typically is of the order of $1 \cdot \lambda \times 1 \cdot \lambda \times K \cdot \lambda$ [3],
9 where λ is the wavelength, and K denotes a constant determined by the transducer geometry (typical
10 values are 5-7). The three-dimensional scanning of the tumor by the focal spot leads to thermal ablation of
11 the entire tumor volume leaving surrounding healthy tissues intact. Acceptance of any promising new
12 therapy and its widespread use in clinical practice depends on the accuracy and repeatability of
13 treatments. An accuracy of treatment depends on 1) the accuracy of guidance of the focal spot of the
14 heating beam [4-7], 2) the accuracy of characterization of the acoustic field applied [8], and 3) the
15 accuracy of controlling of the ultrasound energy delivered [9-11]. Biological effects induced in
16 tissues exposed to the high intensity focused ultrasound beams are typically the result of heating
17 and mechanical effects caused by inertial cavitation.

18 The main objective of this study was to design, manufacture and test a spherical ultrasound
19 annular array transducer suitable for preclinical studies on efficacy of thermal ablation and of tested
20 anti-cancer drugs activated by HIFU beams in the treatment of a variety of solid tumors implanted
21 to various organs of small animals at the depth of the order of 1-2 cm under the skin. The transducer
22 testing consisted of examining the impact of geometry and the acoustic parameters of each beam
23 generated on location and extent of a local necrotic lesion induced within a tested tissue: 1) average
24 acoustic power, 2) focal length, and 3) exposure time. The results of these studies were necessary to
25 assess the feasibility of application of such beams for preclinical studies on small animals as well as
26 to explain the characteristics of thermal lesions formed in the tested tissue *ex vivo*.

1 **2. Materials and methods**

2 To generate the heating beams of the selected acoustic power and different focal lengths we
3 designed and built the spherical 7-element annular phased array transducer. To measure temperature
4 rises induced locally in the tested tissue sample by the heating beams the custom-made
5 experimental setup was designed and constructed. To visualize the thermal lesions formed within
6 the tissue an ultrasound scanner equipped with a linear imaging probe as well as a magnetic
7 resonance scanner were used. Each tissue sample was exposed to three parallel HIFU beams of the
8 same: 6W, or 12W, or 18W, average acoustic power and 25mm, 30mm, and 35mm focal lengths.

9 *2.1. HIFU transducer*

10 Both, the pulsed nonlinear acoustic pressure and temperature fields were produced by the
11 custom-made, spherical, 7-element annular phased array transducer having an external diameter of
12 29 mm, resonance frequency of 2 MHz and f -number of 2, as shown in Fig. 1.

14 **Fig. 1**

15
16 The transducer was made of Pz26 piezo-ceramics (Meggitt, Kvistgaard, Denmark) exhibiting
17 very low aging rate ($< 1\%$ per time decade) and extremely stable performance (over several years).
18 The transducer was air-backed and had one quarter-wavelength matching layer. Each element of the
19 HIFU transducer had the same radiating surface. All elements generated tone bursts with 20-cycle
20 duration, 0.2 duty-cycle and programmable time delay providing the beam focusing in water at
21 three axial distances 25 mm, 30 mm, and 35 mm from the center of the transducer.

22 *2.2. Experimental setup*

23 The experimental setup along with its scheme and cross-section are shown, respectively in Fig. 2
24 and Fig. 1. All measurements were carried out at 36 °C.

26 **Fig. 2**

1 As shown in Fig. 1 and Fig. 2 a custom-made transmitting electronics (IPPT PAN, Warsaw,
2 Poland) contained seven broadband power amplifiers driven by seven 14-bit 80-MHz AD9717
3 converters (Analog Devices, Norwood, MA, USA) controlled by a programmable Altera Arria
4 EP1AGX FPGA logic system (Altera Corporation, San Jose, CA, USA). The amplifiers excited the
5 elements of the annular phased array transducer to produce the heating beam. The voltage applied to
6 each individual element was adjusted between $89 V_{pp}$ and $150V_{pp}$ to generate focused beams with
7 the same average acoustic power and increasing focal lengths. The acoustic power for each beam
8 was measured using an UPM-DT-1E ultrasound power meter (Ohmic Instruments, St. Charles, MO,
9 USA). Each set of time delays, required to focus the beam energy within the tissue sample at the
10 selected depth, was processed using an Altera Quartus software (Altera Corporation, San Jose, CA,
11 USA). The annular array transducer was mounted rigidly in a wall of a container filled with distilled
12 water of a temperature controlled by an ME AC 190 thermostat (Julabo Laborthechnik GmbH,
13 Seelbach, Germany). The waveform of tone bursts generated by transducer elements were recorded
14 using a TDS3012B digital oscilloscope (Tektronix, Beaverton, USA).

15 Pulsed HIFU beams were generated by the annular phased array transducer designed, as shown
16 in Fig. 2. The tone bursts propagated through a two-layer media system consisting of a 15-mm layer
17 of water and a 40-mm layer of pork loin. The thickness of the water layer was selected using our
18 nonlinear propagation model [12] in water as the axial distance from the transducer used at which
19 the amplitude of the second harmonic component starts to be discernible. As shown in previous
20 publication [13] this distance is constant and independent on the source pressure level providing
21 formation of weak or moderate nonlinear fields. To provide an uniform pressure distribution on the
22 surface of the annular array transducer its rings had the same radiating aperture area as the central
23 disk. The focal length of each HIFU beam was controlled electronically by using programmable
24 time delays to the pulsed excitation of the transducer elements. A set of time delays for each focal
25 length was determined by measurements of pressure waveforms generated in water by both, the
26 central disc and consecutive rings using a calibrated S/N 1661 needle hydrophone (Precision

1 Acoustics, Dorchester, UK). The axial position of the maximum heating spot and exposure time
2 needed to locally heat the tissue to induce necrosis, corresponding to a 56 °C temperature, were
3 determined from measurements of temperature by TP-201 thermocouples (Czaki Termo-Product,
4 Raszyn, Poland) placed along the acoustic axis of each HIFU beam. After exposure of each tissue
5 sample to three HIFU beams with the same acoustic power and different focal lengths the necrotic
6 lesions within the tissue at three depths were visualized using both, a Sonix Touch ultrasound
7 scanner (Ultrasonix, British Columbia, Canada) and a Biospec 70/30USR magnetic resonance
8 imaging system (Bruker BioSpin Corporation, Billerica, MA, USA). Consequently, the location and
9 extent of the necrotic lesions was estimated and compared with those predicted using numerical
10 model. The experimental verification of the obtained results was carried out optically with a digital
11 caliper after cutting the tissue sample along the plane containing the three axes of the HIFU beams
12 used.

13 *2.3. Acoustic pressure/intensity field characterization*

14 The beam patterns for the transducer used were characterized numerically and measured in
15 water at room temperature in free-field conditions using a S/N 1661 calibrated 0.2 mm needle
16 hydrophone (Precision Acoustics, Dorchester, Dorset, UK). The initial (source) and focal (in the
17 focal plane) pressure amplitudes were determined from predicted spatial acoustic pressure
18 distributions using our nonlinear propagation model [12] in water and then their fitting to those
19 measured for each beam used. For the beams with the same 6W, or 12W, or 18W acoustic power
20 and 25mm, 30mm, and 35 mm focal lengths the source pressure was found to be equal to 0.369
21 MPa, 0.522 MPa and 0.639 MPa with an uncertainty of about $\pm 4.4\%$ and the initial intensity I_{SATA}
22 of the beam was found to be equal to 0.9 W/cm², 1.8 W/cm², and 2.7 W/cm² with an uncertainty of
23 about $\pm 9\%$, respectively. The focal pressure was found to be equal to 8.4 MPa, 6.8 MPa and 5.5
24 MPa for 6W beams, 12.8 MPa, 10.5 MPa and 8.5 MPa for 12W beams and 17.2 MPa, 14.2 MPa
25 and 11.7 MPa for 18W beams, respectively.

1 The focal intensity I_{SATA} for each beam produced within the tested tissue was determined from
2 numerical simulations of spatial pressure distributions in the beams propagating in the two-layer
3 media system: water/tissue (15mm/40mm) using our nonlinear propagation model [12] required the
4 following input parameters whose values were taken from literature: the pork loin density $\rho_0 = 1060$
5 kg/m^3 [14], sound velocity $c = 1620 \text{ m/s}$ [15], attenuation coefficient $\alpha = 11 \cdot 10^{-6} \text{ Np/(m}\cdot\text{Hz}^b)$ [15],
6 power index of attenuation dependence on frequency $b = 1$ [16], nonlinearity parameter $B/A = 8$
7 [17] and thermal conductivity $K_t = 0.52 \text{ W/(m}\cdot\text{°C)}$ [18]. As mentioned above, each tissue sample
8 was exposed to three parallel HIFU beams with the same average acoustic power and different focal
9 lengths. The distance between axes of the beams was chosen to be 10 mm (in some cases 3mm).
10 The beams were focused within each sample at 10mm, 15mm, and 20mm depths under the
11 water/tissue interface. The calculated values of the focal intensity I_{SATA} in three beams used were
12 found to be equal to 410 W/cm^2 , 260 W/cm^2 , and 170 W/cm^2 for 6W beams; 940 W/cm^2 , 630
13 W/cm^2 , and 410 W/cm^2 for 12W beams, and 1690 W/cm^2 , 1150 W/cm^2 , and 780 W/cm^2 for 18W
14 beams, respectively.

15 2.4. *Temperature measurement protocol*

16 Measurements of temperature induced locally in each pork loin sample by three parallel HIFU
17 beams with the same acoustic power and increasing focal length were carried out using the
18 experimental setup shown in Fig. 1. Both, the ultrasound and magnetic resonance imaging of the
19 three necrotic lesions formed within each tissue sample as well as its cutting were performed after
20 exposure to the three heating beams as is shown in Fig. 3.

21

22

Fig. 3

23

24 Each pork loin sample was inserted in a cylindrical holder and immersed in a water bath with a
25 controlled temperature of 36 °C . The HIFU beams were focused electronically within each tissue
26 sample, successively at the depth of 10 mm, 15 mm and 20 mm below the water/tissue interface. All

1 pieces of pork loin from which the samples were prepared were fresh. They were bought in a meat
2 factory store. Each sample was degassed and inserted in a cylindrical holder with a 40-mm inner
3 diameter and 40-mm height. The holder had a 20- μ m-thick, transparent for sound, Mylar windows
4 stretched tightly over each end to prevent bowing of the water/tissue interface. During experiments
5 the windows stayed parallel to each other and perpendicular to acoustic axes of the beams. The
6 design and construction of the experimental setup ensured that errors arising due to HIFU beam
7 refraction were minimized. The lesions were formed at central, left, and right region of each sample
8 by moving laterally the holder between exposures at 3 axial positions: central - coaxial with the
9 transducer, left, and right, spaced apart by 10 mm to minimize overlapping of the beams penetrating
10 into the tissue.

11 As already mentioned, the path-length of the pulse propagation in water before penetrating into
12 the tissue was selected from axial harmonic pressure distributions calculated for nonlinear HIFU
13 beams produced in water. For the heating beams used here this distance was found to be 15 mm.
14 Selection of thickness of the water layer in two-layer media system used was done to maximize the
15 effect of the harmonic waves generation in the focal region. Their attenuation increase nonlinearly
16 with frequency being one of the reasons of thermal effects induced within tissue.

17 Temperature rises induced in each tested tissue sample by three HIFU beams used were
18 measured by TP-201 thermocouples (Czaki Termo-Product, Raszyn, Poland) with a diameter of 0.2
19 mm. The thermocouples were placed inside the tissue sample along the heating beam axis using thin
20 0.5 mm, hypodermic needles inserted through a cover of the water container in steps of 5 mm,
21 providing their exact position on the axis of each beam used. The uncertainty of position of the
22 thermocouples was ± 0.5 mm. Due to a small diameter their influence on measurement results were
23 considered negligible. The temperature rise detected by each thermocouple was recorded in steps of
24 1 second by USB-TEMP unit (Measurement Computing, Norton, USA) and transferred to the PC
25 memory. To process data obtained and to visualize the temperature-time plots a TracerDAQ
26 software (MicroDAQ.com Ltd, Contoocook, NH, USA) was used. The maximum temperature rise

1 determined the position of the maximum heating spot, which, in turn, determined the depth of
2 location of the thermal lesion. Example of the temperature rises $\Delta T(t)$ induced in the tested tissue
3 during its exposure to three HIFU beams and measured by thermocouples placed along the acoustic
4 axis of each beam is shown in Fig. 4.

5 **Fig. 4**

6
7 After three exposures the necrotic lesions induced in each tissue sample were visualized using
8 both, the ultrasound and magnetic resonance imaging techniques. Then, the tissue sample, being
9 inside the holder, was sliced carefully along the plane containing three beam axes to make the
10 lesions optically visible and to verify manually their location and dimensions with accuracy within
11 ± 0.1 mm using digital caliper.

12 *2.5. Ultrasound and magnetic resonance imaging of necrotic lesions*

13 For ultrasound imaging of the necrotic lesions a Sonix Touch scanner (Ultrasonix, British
14 Columbia, Canada) equipped with a L14-5/38 linear phased array probe operating at a 10 MHz
15 frequency was used. Ultrasound imaging was done immediately after three exposures of each
16 sample. Magnetic resonance imaging was done 30 ± 5 minutes after three exposures using Biospec
17 70/30USR high-field (7T) magnetic resonance scanner for small animals (Bruker BioSpin
18 Corporation, Billerica, MA, USA).

19

20 **3. Results and discussion**

21 Quantitative analysis of spatial acoustic pressure/intensity distributions in the pulsed nonlinear
22 beams produced in the two-layer media system: water/tissue and predicted using our nonlinear
23 propagation model allowed to show that for the beams with the same acoustic power and increasing
24 focal length the maximum pressure decreases, while the full width half maximum (FWHM)
25 dimensions of the ellipsoidal focal volume increases. For example, for 6W beams the maximum
26 pressure decreased from 8.5 MPa to 5.5 MPa, while dimensions of the ellipsoidal focal volume

1 increased from 1.1mm x 1.1mm x 6.8mm for the beam of a 25mm focal length to 1.4mm x 1.4mm
2 x 11.2mm for the beam of a 35mm focal length. It means that focal volume increased about 3 times.
3 Meanwhile, for 3 times more powerful (18W) beams the maximum pressure decreased from
4 17.2MPa to 11.7MPa, while ellipsoidal focal dimensions increased from 0.9mm x 0.9mm x 6.4mm
5 for the beam of 25-mm focal length to 1.1 mm x 1.1 mm x 10 mm for the beam of the 35-mm focal
6 length. So, focal volume increased about 2 times. Comparing the dimensions of the focal volume
7 for the beams with the same focal lengths and increasing power we have shown that the higher the
8 acoustic power, the smaller sizes of the focal volume. This is probably due to the shorter exposure
9 time necessary for beams of the greater power to heat tissue locally to 56 °C, which in turn leads to
10 a reduced heat diffusion.

11 Quantitative analysis of the temperature rises, induced locally in each pork loin sample during
12 its exposure to the three HIFU beams and measured by thermocouples, revealed that for 6W beams
13 the axial positions of the maximum heating within tissue were approximately 2.5 mm shallower
14 under water/tissue interface than those resulting from the geometry, i.e. 10mm, 15mm, and 20mm,
15 respectively. In the case of 18W beams the axial positions of the maximum heating corresponded to
16 those resulting from the geometry. For the beams of 12W the axial position of the maximum
17 heating for the beam with 25-mm focal length was found at the same depth as resulting from the
18 geometry, meanwhile, as for the beam with 30-mm focal length it was about 2.5 mm shallower
19 under the tissue penetration surface (between 10mm and 15mm), similar as for the beam with 35-
20 mm focal length (between 15mm and 20mm). This is illustrated in Fig. 4. The exposure time for
21 each beam used was determined from the temperature-time $\Delta T(t)$ relationship as the duration
22 required to heat locally the tested tissue to 56 °C leading to the formation of the necrotic lesion.

23 The measurement results allowed to show that the larger the focal length of the beam, the longer
24 the exposure time is required to form the necrotic lesion (to heat locally the tested tissue to 56 °C)
25 as shown in Fig. 4. This results from the lower focal intensity for the beams with the larger focal
26 length and from increased heat diffusion during longer exposure needed to induce necrosis. This, in

1 turn, leads to expansion of the heated tissue volume and, thus, to increased extension of the necrotic
2 lesion. Considering that the essence of thermo-ablative anti-tumor HIFU therapy involves the rapid
3 (less than 3 seconds) heating of a small volume within a tumor to a temperature of 56 °C and
4 scanning the beam focus throughout the entire tumor we showed that only the beams with an output
5 exceeding 12W were able to meet this condition. As can be seen from Fig. 4 the exposure time
6 needed to heat locally the tested tissue to 56 °C varied between 2 second for the beam of 25-mm
7 focal length and 3.8 seconds for the beam of 35-mm focal length.

8 On the ultrasound images of the axial cross-section (xz plane) of each sample after its exposure
9 to the three HIFU beams with the same acoustic power and increasing focal lengths, the necrotic
10 lesions were visible, although their contours were not clearly defined because of blurry edges, as
11 shown in Fig. 5. The sizes of thermal lesions visible on the ultrasound images were larger than
12 those measured by caliper. Probable cause of this is insufficient rate of temperature increase to form
13 a clear boundary between necrotic lesion and undamaged tissue structures as well as to induce in
14 tissue gas bubbles improving the contrast of ultrasound imaging due to the induction of inertial
15 cavitation.

16
17 **Fig. 5**
18

19 However, after cutting each sample along the xz plane, the necrotic lesions with clearly outlined
20 edges were visible to the naked eye, as shown in Fig. 6.

21
22 **Fig. 6**
23

24 The magnetic resonance images of axial cross-sections of each tissue sample in planes parallel
25 to xz plane and spaced apart by 0.5 mm showed much more clearly defined boundaries of the
26 necrotic lesions, as can be seen Fig. 7.

Fig. 7

Optical visualization and measuring of three thermal lesions allowed to verify experimentally their extent and location under the water/tissue interface. This was done by comparison the location and dimensions of the necrotic lesions measured by digital caliper after cutting each sample with those predicted numerically as well as with those imaged using ultrasound and magnetic resonance imaging techniques. Results of comparison of the calculated sizes of thermal lesions with those measured by the caliper have shown that both, the nonlinear propagation and bio-heat transfer models predict well the acoustic pressure and temperature fields produced in the two-layer media system used. The agreement between the calculation results and measurement data was within $\pm 9\%$. The sizes of thermal lesions visible on the ultrasound images were not in good correlation with those measured by caliper, although their location corresponded to measured ones, as shown in Fig. 6. Meanwhile, the location and extent of thermal lesions visible on the magnetic resonance images fully corresponded to those measured by caliper, as demonstrated in Fig. 7.

4. Conclusions

In conclusion, we have shown, that it is feasible to manufacture spherical annular phased array transducer with electronically adjustable focal length suitable for preclinical studies of efficacy of tested, anti-cancer, ultrasound-activated drugs in the treatment of a variety of primary solid tumors localized in various organs of small animals at the depth of the order of 1-2 cm under the skin. Our experiments revealed the encouraging results showing the feasibility of inducing within tissues local necrotic lesions using the designed, custom-made, spherical, 7-element annular array transducer generating HIFU beams with electronically adjustable focal length. The necrotic lesions with clearly outlined edges were formed within pork loin tissue *ex vivo* at desired depths starting from the beams of 12W acoustic power. Optical inspection of the axial cross-section of each sample

1 exposed to the three HIFU beams with the same acoustic power and increasing focal lengths
2 confirmed that the location and extent of the local necrotic lesions induced within the tested tissue
3 are in good correlation with those predicted by numerical modeling and verified using both, the
4 ultrasound and magnetic resonance imaging techniques as well as optical revision using digital
5 caliper after slicing the tissue sample.

6 The necrotic lesions had clearly outlined edges. On the basis of measurement data we showed
7 that for exposure parameters used, the location and extent of the necrotic lesions induced in the
8 tested tissue *ex vivo* strongly depend on the acoustic power, focal length and exposure time of the
9 heating beam used. This is important for preclinical applications proposed.

10 The theoretical and experimental studies described here indicated that pulsed HIFU beams with
11 electronically adjustable focal length, generated by the annular array transducer designed can be
12 used as an effective, non-invasive tool useful for both, 1) the thermo-ablative treatment of primary
13 solid tumors localized within various organs of small animals at the depths of 1-2cm under the skin
14 and 2) their treatment based on delivery of anti-cancer drugs activated by HIFU beams. However,
15 further studies are needed to test the developed transducer on solid tumors *in vivo* implanted to
16 small animals.

17

18

19 **Acknowledgments**

20 The financial support of National Science Centre of Poland (Project 2011/01/B/ST7/06735) is
21 gratefully acknowledged.

22

23

24

25

26

1 **References**

- 2 [1] ter Haar G. Therapeutic applications of ultrasound. *Prog Biophys Mol Biol* 93: 111-129, 2007.
- 3 [2] Miller D, Smith N, Bailey M, Czarnota G, Hynynen K, Makin I. Overview of therapeutic
4 ultrasound applications and safety considerations. *J Ultrasound Med.* 31(4): 623-634, 2012.
- 5 [3] Ebbini ES and ter Haar G. Ultrasound-guided therapeutic focused ultrasound: Current status
6 and future directions. *Int J Hyperthermia* 31(2): 77-89, 2015.
- 7 [4] Yang R, Sanqhvii NT, Rescorla FJ, Galliani CA, Fry FJ, Griffith SL, Grosfeld JL.
8 Extracorporeal liver ablation using sonography-guided high intensity focused ultrasound. *Invest*
9 *Radiol* 27:796-803, 1992.
- 10 [5] Hutchinson E, Dahleh M, Hynynen K. The feasibility of MRI feedback control for
11 intracavitary phased array hyperthermia treatments. *Int J Hyperthermia* 14: 39-56, 1998.
- 12 [6] McDannold NJ, King RL, Lolesz FA, Hynynen KH. Usefulness of MR imaging-derived
13 thermometry and dosimetry in determining the threshold for tissue damage induced by
14 thermal surgery in rabbits. *Radiology* 216: 517-523, 2000.
- 15 [7] Kaye EA, Chen J, Pauly KB. Rapid MR-ARFI method for focal spot localization during
16 focused ultrasound therapy. *Magn Reson Med* 65: 738-743, 2011.
- 17 [8] ter Haar G, Shaw A, Pye S, Ward B, Bottomley F, Nolan R, Coady AM. Guidance on
18 reporting ultrasound exposure conditions for bio-effects studies. *Ultrasound in Med. Biol.*
19 37 (2): 177-183, 2011.
- 20 [9] Fry FJ, Kossof G, Eggleton RC, Dunn F. Threshold ultrasonic dosages for structural
21 changes in the mammalian brain. *J Acoust Soc Am* 48: 1413-17, 1970.
- 22 [10] Frizzel LA, Threshold dosages for damage to mammalian liver by high intensity focused
23 ultrasound. *IEEE Trans Ultrason Ferroelectr Freq Control* 35: 578-81, 1988.
- 24 [11] Sapareto SA, Dewey WC. Thermal dose determination in cancer therapy. *Int J Radiat*
25 *Oncol Biol Phys* 10: 787-800, 1984.
- 26 [12] Wójcik J, Nowicki A, Lewin PA, Bloomfield PE, Kujawska T, Filipczyński L. Wave

- 1 envelopes method for description of nonlinear acoustic wave propagation. *Ultrasonics* 44:
2 310-329, 2006.
- 3 [13] Kujawska T, Nowicki A, Lewin PA. Determination of nonlinear medium parameter
4 B/A using model assisted variable-length measurement approach. *Ultrasonics* 51(8): 997-
5 1005, 2011.
- 6 [14] Duck FA. *Physical properties of tissue: a comprehensive reference book*. Academic Press,
7 London, p. 139, 1990.
- 8 [15] Koch T, Lakshmanan S, Brand S, Wicke M, Raum K, Moerlein D. Ultrasound velocity and
9 attenuation of porcine soft tissues with respect to structure and composition: I. Muscle.
10 *Meat Science* 88: 51-58, 2011.
- 11 [16] Nassiri DK, Nicholas D, Hill CR. Attenuation of ultrasound in skeletal muscle,
12 *Ultrasonics* 17: 230-232, 1979.
- 13 [17] Law WK, Frizzell LA, Dunn F. Determination of the nonlinearity parameter B/A
14 of biological media. *Ultrasound in Med Biol* 11: 307-318, 1985.
- 15 [18] Kujawska T, Secomski W, Kruglenko E, Krawczyk K, Nowicki A. Determination of
16 tissue thermal conductivity by measuring and modeling temperature rise induced in
17 tissue by pulsed focused ultrasound. *PlosONE* 9(4): 1-8, 2014.

1 **List of figure captions**

2 **Fig. 1.** Scheme and cross-section of the experimental setup. The cylindrical chamber with the tissue
3 was moved horizontally to the left and right by 10mm (in some case by 3mm).

4 **Fig. 2.** Photo of the experimental setup for measuring temperature rises induced in the tested tissue
5 during exposure to focused ultrasound.

6 **Fig. 3.** Scheme of axial cross-section of a tissue sample exposed to three parallel HIFU beams of the same
7 acoustic power and increasing focal length. Locations of thermocouple tips (dots) and thermal lesions
8 (ellipsoids) formed during exposure are shown.

9 **Fig. 4.** Tissue temperature measured at penetration depths of 5mm (red), 10mm (blue), 15mm (black),
10 20mm (green), and 25mm (orange) for 12W beams of 25mm (left), 30mm (middle) or 35mm (right) focal
11 length.

12 **Fig. 5.** Ultrasound images of the tested tissue sample before (A) and after (B) exposure to the three
13 parallel HIFU beams of the same, 12W, acoustic power and 25mm, 30mm, and 35mm focal length.
14 Thermal lesions induced at 10mm, 15mm, and 20mm penetration depths are indicated by arrows.

15 **Fig. 6.** The axial cross-sections of tested tissue samples exposed to the three parallel HIFU beams of
16 the same: 6W (left) or 18W (right) acoustic power and 25mm, 30mm, or 35mm focal length. The
17 beams spaced apart by 10 mm (left) or 3 mm (right) are shown.

18 **Fig. 7.** Magnetic resonance images (T1) of axial cross-sections for the tested tissue exposed to three
19 parallel HIFU beams of 12W acoustic power and 25mm, 30mm, or 35 mm focal length. Four
20 parallel slices spaced apart by 0.5 mm are shown. Necrotic lesions are indicated by arrows.

Figure 1

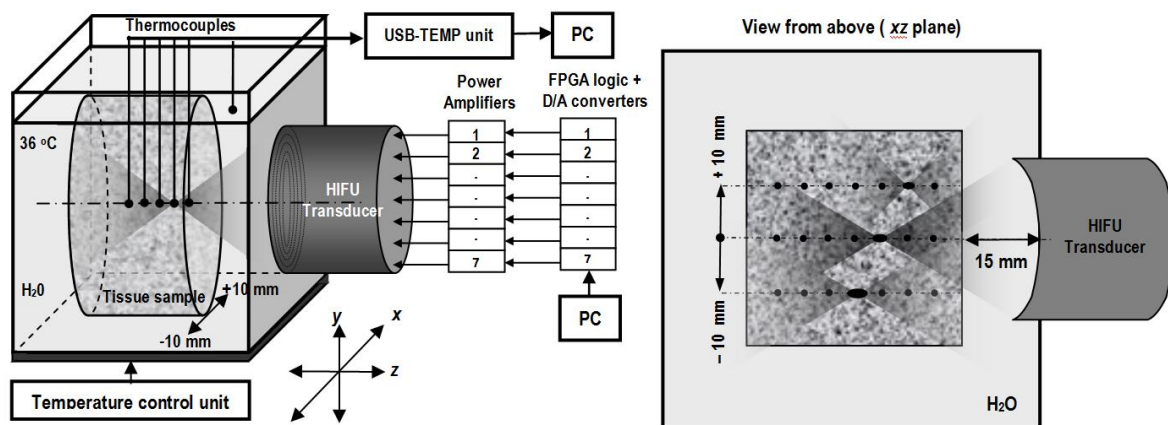


Figure 2

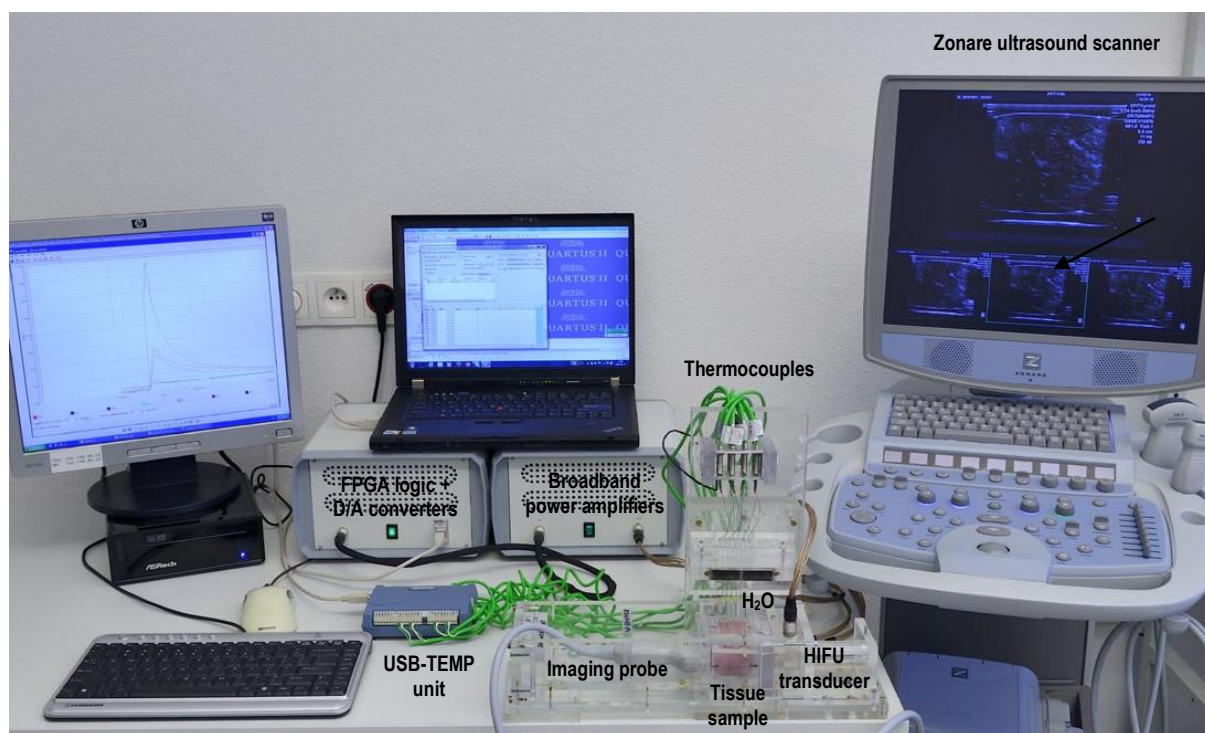


Figure 3

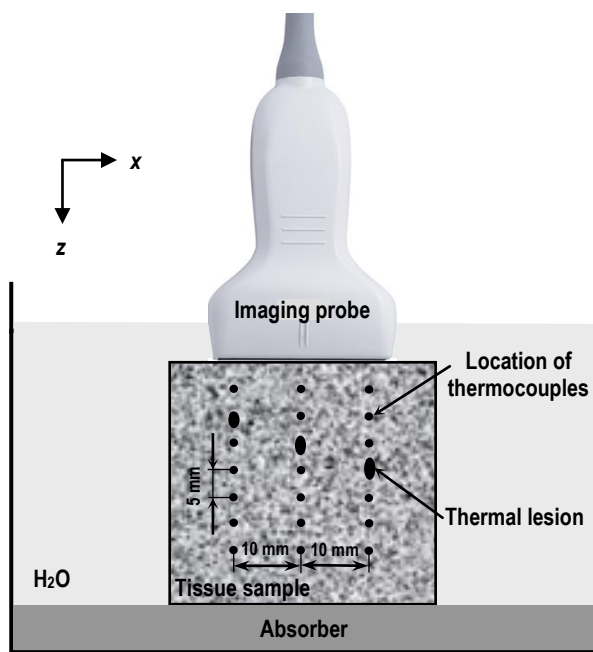


Figure 4

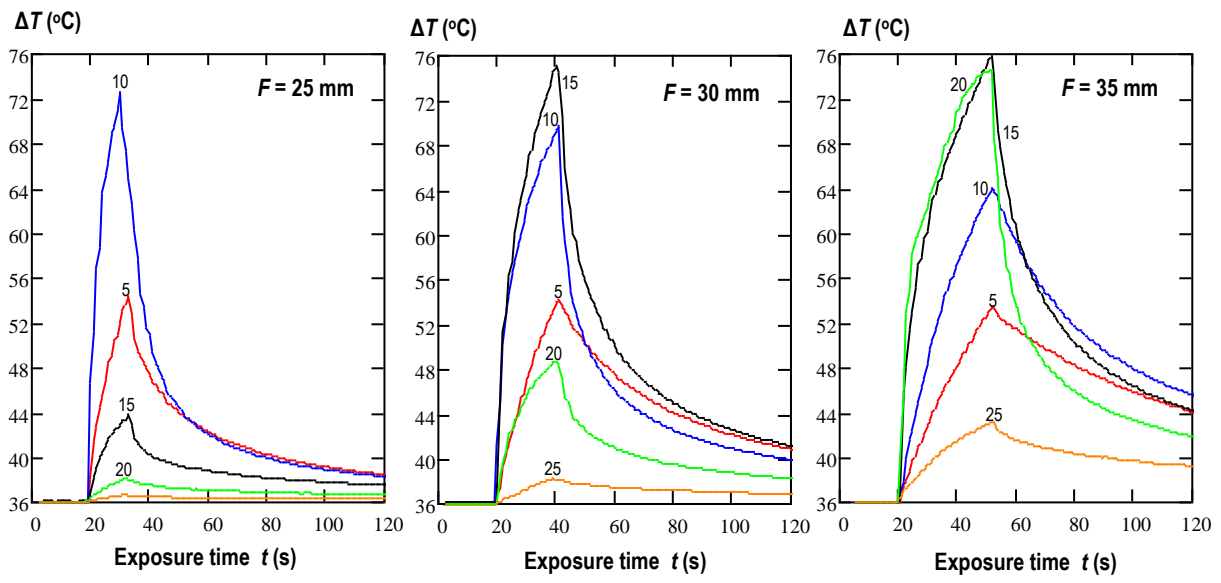
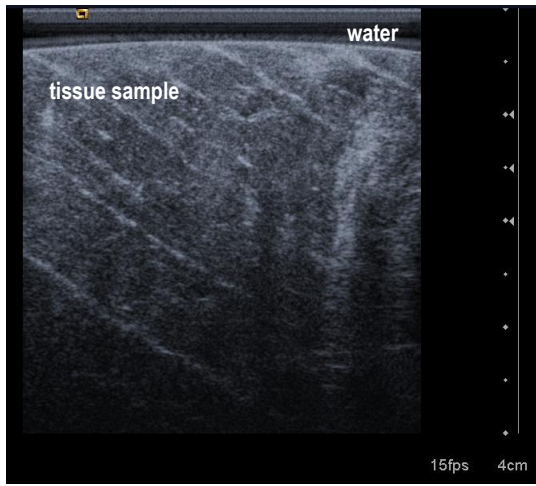


Figure 5



A



B

Figure 6

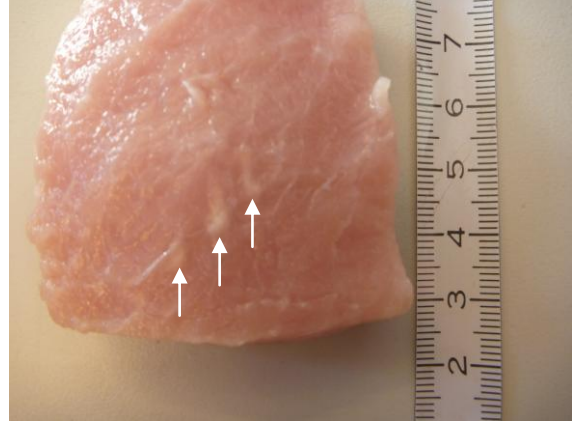
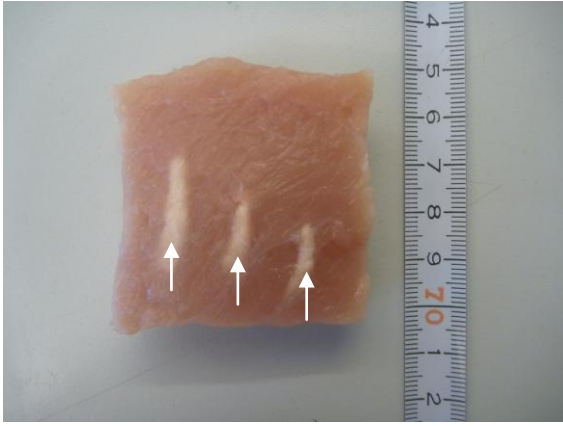


Figure 7

